Scientia Iranica, Vol. 12, No. 2, pp 167–177

SCIENTIA IRANICA

Behavior of Gravely Sand Using Critical State Concepts

S.M. Hosseini*, S.M. Haeri[1] and D.G. Toll[2]

A series of consolidated undrained triaxial tests were performed in order to understand the behavior of a gravely sand. The material was selected from Tehran alluvium and is classified as gravely sand in the Unified Soil Classification System. Critical state concepts were used for interpretation of the behavior of the soil. The critical state line in $q - p'$ space was reasonably unique. However, it was not possible to define a unique critical state line in e-ln p' space. The overall scatter, in the critical state line for the gravely sand studied, was $\pm$ 0.04, in terms of void ratio. Two reasons can be identified for this scatter. The first reason is the inevitable error in void ratio calculation and the second is that the behavior of this material, even at a critical state, is fabric and structure dependant. On the basis of these tests, it has been concluded that, for this material, a critical state zone with upper and lower limits can be defined. Nevertheless, a unique boundary surface can be defined by presenting the data in normalized stress space.

INTRODUCTION

The main objective of this paper is to examine the critical state concept for gravely sands. Previous studies have, generally, examined the critical state on uniformly graded sands or silty sands. The soil tested here is gravely and more widely graded when compared to those that have been reported in the literature.

The concept of a critical void ratio has been used to explain the behavior of soil since 1936. Critical void ratio has two definitions in the literature. Casagrande [1] defined critical void ratio as the void ratio at which sand does not change in volume when subjected to shear. Taylor [2] defined critical void ratio as the void ratio at which prevention of volume change leads to no strength change. These two definitions are consistent, as the first definition applies to drained conditions and the second to undrained conditions. Roscoe et al. [3] showed that the concept of a critical void ratio is valid for clays as well as for sands. The paper by Roscoe et al. [3] was the starting point for the development of critical state soil mechanics. The concept of the critical state is illustrated, schematically, in Figure 1.

There have been discussions in the literature concerning the ultimate behavior of sands, to differentiate between "critical state" and "steady state". Researchers who worked on the behavior of soil using critical state soil mechanics have defined the critical state as follows: "In a drained test, the critical void ratio state can be defined as that ultimate state of a sample at which any arbitrary further increment of shear distortion will not result in any change of void ratio. In an undrained test, the sample remains at a constant void ratio, but, the effective stress, p', will alter to bring the sample into an ultimate state, such that the particular void ratio, at which it is compelled to remain during shear, becomes a critical void ratio" [3]. The following shorter definition was given by Schofield and Wroth [4]: "The critical state is an ultimate condition where a soil element will continue to deform without further change in stresses and volume".

It is normally assumed that the critical state is one in which the initial fabric and structure of the soil is destroyed or rearranged to produce a random fabric. Poulos [5] suggested that such a state of shearing under constant stress and volume can be temporarily achieved (a quasi steady state) but that it is not the

*. *Corresponding Author, Department of Civil Engineering, Sharif University of Technology, P.O. Box 11365/9313, Tehran, I.R. Iran.*

1. *Department of Civil Engineering, Sharif University of Technology, P.O. Box 11365/9313, Tehran, I.R. Iran.*
2. *School of Engineering, University of Durham, Durham, UK.*

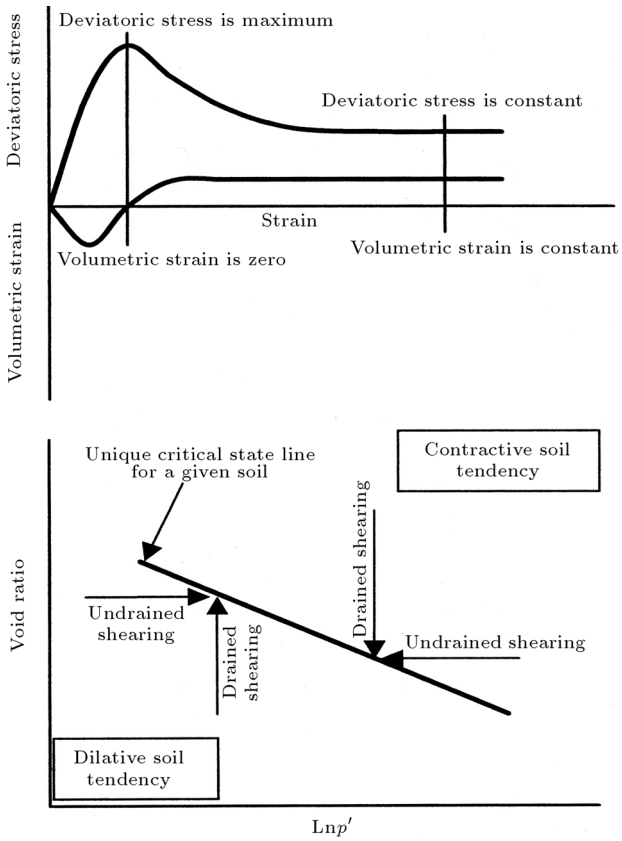

Figure 1. Schematic diagram showing definition of critical state.

true ultimate state. Continued shearing will develop an oriented flow structure when a true state of shearing under constant stresses and volume is achieved. Poulos [5] indicates that these can only be identified when shearing occurs at a constant velocity and, hence, defines the steady state as the following: "The steady state of deformation for any mass of particles is that state in which the mass is continuously deforming at constant volume, constant normal effective stress, constant shear stress and constant velocity".

At critical state, volume change and shear stress are constant but the fabric coinciding with this state may be random or oriented. Poulos emphasizes that, in the steady state, the structure is oriented and deformation velocity is constant. Considering these different definitions of critical state and steady state as mentioned above, one can conclude that the definitions of both concepts are similar, based on constant volume, constant effective mean stress and constant shear stress. However, Poulos emphasizes the constant velocity and structure orientation for steady state. He states that, if the velocity of deformation were zero or not constant, the specimen would not be in the steady state condition.

Some researchers differentiate between critical and steady states according to the testing method. Critical state has, generally, been observed on drained, strain-rate-controlled tests. Steady state has been observed in undrained tests, usually on loose (contractive) samples [6]. Examples of the steady state of deformation have been observed in undrained tests on saturated loose sand during liquefaction. Chu [7] suggests that, for contractive soils, the critical state is the ultimate state in a drained test and the steady state is the ultimate state in an undrained test. However, Poulos [5] stated that the steady state could be achieved in both drained and undrained tests.

The critical state was used in this paper, defined as the state observed in undrained triaxial tests when constant deviator stress and mean effective stress have been achieved. This definition may represent a "quasi steady state" condition, such that, with further shearing, an oriented flow structure would be developed. However, as Poulos [5] states, it may not be possible to get to the steady state in triaxial tests, where there are limitations on the applied maximum strain.

CRITICAL/STEADY STATE FOR SANDS

Critical state and steady state concepts have been investigated for a range of geotechnical materials (e.g., sand, silty sand, clay and soft rock). Early work focused on clays, but during the last decade, attention has been given to sands. The following pieces of work are of particular significance.

Been et al. [6] examined the critical state for a fine to medium, uniformly graded quartzite sand. They showed that the critical and steady states are equal to and independent of a stress path, a sample preparation method and initial density. The overall scatter in the critical state line for the sand studied was in the range of $\pm$ 0.01, in terms of void ratio, at a stress level less than 1000 kPa. They suggested that for real sands with more variable intrinsic properties, the scatter might be much larger.

Riemer and Seed [8] examined the effect of several factors on the apparent position of the steady-state line. They studied Monterey # 0 sand, which is a uniform, clean and fine beach sand. Their results showed that the stress level to which samples were consolidated prior to shearing could affect the undrained strength. However drainage condition did not appear to affect the steady state relationship. From test results in simple shear and triaxial (compression and extension), it appeared that the stress path itself was not the important factor, but, that the mode of deformation (i.e., strain orientation) could have a significant impact on the effective stress condition achieved at large strains.

Verdugo and Ishihara [9] carried out triaxial tests on Toyoura sand under both undrained and drained conditions. The results indicated that the quasi steady

state was slightly affected by the initial mean stress, whereas the steady state was unaffected by the initial mean stress. Furthermore, the locus of the ultimate state achieved through drained conditions of loading, was shown to be coincident with the steady state line evaluated by means of undrained tests. They suggested that for a homogeneous soil mass, the steady state line is a unique reference line unaffected by the type of soil deposition and initial state condition of density and pressure.

Chu [7] examined critical state and other similar concepts for Sydney sand, a uniformly graded quartz sand. He suggested that the critical state curve is independent of the initial void ratio of the soil. The other states i.e., the phase transformation state, the characteristic state and the steady state, were closely related to the critical state. For contractive soils, all states became the same and described the behavior at the ultimate (or failure) state. For dilative soils, the phase transformation state and the characteristic state were the same.

Fourie and Papageorgiou [10] examined the steady state for Merriespruit gold tailings. Four particle size distributions of Merriespruit tailings were tested to determine the influence of the fines content on the position of the steady state line. Test results showed that tailings with the greatest percentage of fines gave a steady state line that plotted above all the others. They pointed out that it is impossible to define void ratio at steady state conditions to the accuracy often quoted in the literature. It is preferable to accept that some error is inevitable and to present a confidence zone with upper and lower limits to the steady state line.

Yamamuro and Lade [11] examined steady state concepts for Nevada silty sand, which included particles between 0.3 mm and 0.075 mm. The sand was combined with 7% nonplastic Nevada fines. Results from undrained tests with different initial void ratios produced different steady state lines. Unique steady state lines may, therefore, not always exist for silty sand.

Mooney et al. [12] examined the uniqueness of the critical state for a sand. Their results indicated that the relationship between shear stress, q, and mean effective stress, p', at critical state, was unique. However, there was not a unique critical state void ratio for a given mean effective stress.

Test results reported by Konrad [13-15] on two sands, showed that the mean steady state line (F line), commonly used for the evaluation of liquefaction potential, was not uniquely related to void ratio for a given sand. Rather, the tests revealed that initial effective confining stress also influenced the undrained behavior of granular material. Furthermore, the tests confirmed the existence of upper and lower limits of the F line, which were defined as UF and LF lines, respectively.

It seems that, for current state-of-the-art, several basic questions, previously mentioned by Been et al. [6], have not yet been answered. These questions include the following:

a) Is the Critical/Steady State unique for any particular sand, including silty sand and gravely sand, or does it depend on the initial fabric, structure and stress path of the test? Are the effects of these factors the same for all sands, including gravely sand?

b) From a practical standpoint, are the critical and steady states the same?

c) What is the general shape of the critical /steady state over a wide range of void ratio and stresses?

d) How precisely and repeatedly can the critical /steady state be measured?

This paper adds to the range of sands for which the critical state/steady state has been investigated, particularly towards a coarser (gravely) soil, and gives a few directions toward finding the answers to some of these questions.

EXPERIMENTAL PROGRAM

In order to investigate the behavior of gravely sand and to define the critical state for this material, a total of 29 triaxial tests were performed under isotropically consolidated undrained conditions. The tests were carried out under five different confining pressures, between 25 kPa and 500 kPa. Tests were performed on samples compacted to two relative densities, 50% and 70%. A summary of the tests performed is shown in Table 1.

Test Material

Material for this research was selected from Tehran alluvium. Tehran alluvium is highly variable in grading and degree of cementation. The range of cementation is from completely uncemented to strongly cemented and the range of gradation is from gravel and boulders in the north of the deposit to clay and silt in the south. This research was performed on the alluvium from a region of Tehran where its gradation is in the range of gravely sand. The grain size distribution of this material is shown in Figure 2 and is comprised of 6% fines, 49% sand and 45% gravel. The shape of the particles is subrounded. The properties of gravely sand, which is classified as SW-SM in the Unified Soil Classification System, are tabulated in Table 2.

Table 1. Summary of the testing program.

Test No.	Confining Pressure, (kPa)	Relative Density After Consolidation (%)	Void Ratio After Consolidation e_c	Critical State Condition	
				Effective Mean Stress p' (kPa)	Deviatoric Stress q (kPa)
CU1	25	54.7	0.444	109.3	175.3
CU2	25	75.7	0.386	134.4	223.4
CU3	25	69.9	0.402	234	390
CU4	25	75.7	0.386	131.4	209
CU5	50	51.4	0.453	187.5	323.6
CU6	50	50.4	0.456	190.6	308.5
CU7	50	52.1	0.451	111.4	176
CU8	50	74.6	0.389	137.3	227.4
CU9	50	77.1	0.382	130.8	232.7
CU10	50	68.4	0.406	287.4	488.8
CU11	50	76.0	0.385	215.9	364.7
CU12	100	55.8	0.441	239.3	411.3
CU13	100	55.4	0.442	112.6	182
CU14	100	59.0	0.432	91.6	147.5
CU15	100	59.7	0.430	194.9	317.5
CU16	100	60.5	0.428	138	226.5
CU17	100	75.0	0.388	178	290
CU18	100	74.2	0.390	287	472.3
CU19	100	72.1	0.396	162.3	264
CU20	300	62.3	0.423	410.4	674.8
CU21	300	53.6	0.447	318.2	501.8
CU22	300	76.0	0.385	208.6	319.2
CU23	300	85.1	0.360	270.4	440.6
CU24	300	78.6	0.378	439	734.1
CU25	400	57.6	0.436	286.5	430.6
CU26	450	51.0	0.454	418.4	671.2
CU27	450	56.5	0.439	295.1	457.7
CU28	450	78.2	0.379	548.4	847.5
CU29	500	89.8	0.347	354.7	565.3

Table 2. Physical properties of gravely sand.

Effective Grain Size D_{10}	Median Grain Size D_{50}	Coefficient of Uniformity C_u	Coefficient of Curvature C_c	Specific Gravity of Solids, G_s	Maximum Void Ratio e_{max}	Minimum Void Ratio e_{min}
0.2 mm	4 mm	28	1.8	2.6	0.595	0.319

Test Procedure

A standard triaxial apparatus was used for testing the gravely sand samples. Samples, 100 mm in diameter and 200 mm in height, were prepared in split molds mounted on the lower platen of the apparatus. Samples were tamped into the mold in eight equal layers to achieve the desired void ratio. The material forming each layer was first dried and weighed and 9.5% water (equal to the optimum moisture content of the material) was added. The samples were saturated by flushing with carbon dioxide gas before flushing with de-aired water. The process of saturation was followed by increasing back pressure until a B value greater than 0.95 was obtained. During this process, an effective stress of approximately 15 kPa was maintained on the sample. After saturation, samples were isotropically consolidated and were sheared

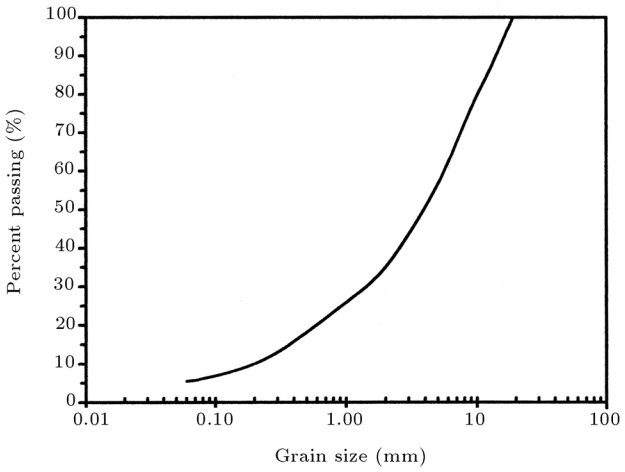

Figure 2. Grain size distribution of the gravely sand.

under strain control at a strain rate of 0.15% per minute.

Membrane Penetration

Triaxial testing devices are employed for a major portion of the engineering investigations on the behavior and strength characteristics of soil. However, for coarse grain soils, as pointed out by many researchers [16-18], during undrained and drained tests on saturated samples, penetration of the flexible rubber membrane into peripheral voids changes and influences pore pressure and volume change measurement, respectively. The membrane penetration effect depends on factors such as effective confining pressure, mean grain size, relative density and membrane thickness. Consolidated undrained triaxial tests have been performed in this research. Therefore, membrane penetration has an effect on the volume change measurement at the consolidation stage and on pore pressure at the shear stage. At the consolidation stage, the equation, proposed by Baldi and Nova [16] for volume change correction, was used as below:

$$V_c = V_0 - \Delta V + V_m, \tag{1}$$

$$V_m = \frac{1}{2}\frac{d_g}{D}V_0\left[\frac{\sigma'_3 d_g}{E_m t_m}\right]^{1/3}. \tag{2}$$

At the shear stage, membrane penetration may have an influence on pore water pressure. Ansal and Erken [17] formulated a correction procedure to calculate the effect of membrane compliance on pore pressure. They showed that pore pressure measurement can be corrected by an amplification factor, which depends on grain size distribution, membrane flexibility, confining pressure, soil compressibility, relative density and sample diameter. Although base soil, in this research, contains coarse grain material, it also has sufficient fine grains, which can cover voids on the peripheral surface of the sample. On the other hand, membrane penetration usually has a significant effect on pore pressure when the soil is at a loose to medium density state. However, in this research, the samples were tested at medium to high relative densities. Two membranes were used during the triaxial tests in this research because the first membrane was usually damaged during the compaction of the soil inside the mold, during sample preparation. An increase in thickness decreases the flexibility of the membrane, resulting in the decreasing effect of membrane penetration. Using 100 mm samples is a good defense against the membrane compliance effect because increasing sample diameter causes a decrease in the membrane compliance effect. With reference to the aforementioned discussion, the membrane effect on pore pressure development during shear has been neglected.

Void Ratio Calculation

Calculation of void ratio forms the basis for the analysis of test results using critical state concepts. Void ratio was calculated by using a dimension of samples. The void ratio was defined as:

$$e = \frac{V}{V_s} - 1. \tag{3}$$

In which V and V_s are, respectively, the total volume after consolidation and volume of solids in the specimen. For a cylindrical sand specimen of height h, diameter d and with a dry weight, m_s, and specific gravity of solids, G_s, Equation 3 can be rewritten as:

$$e = \frac{\pi d^2 h G_s}{4m_s} - 1. \tag{4}$$

Vaid and Sivathayalan [19] have determined that the maximum error in void ratio in this method is:

$$\Delta e = (1+e)\left[\frac{2\Delta c}{c} + \frac{\Delta h}{h} + \frac{\Delta m_s}{m_s} + \frac{\Delta G_s}{G_s}\right], \tag{5}$$

where Δc, Δh, Δm_s and ΔG_s are, respectively, errors in circumference, height, mass and specific gravity measurements. Vaid and Sivathayalan [19] assumed that the error in specific gravity for sand was zero. However, in this research, because gravely sand includes a wide range of grain size and is not uniform in material, one cannot assume ΔG_s to be equal to zero. For this study, the error in measurement of circumference (Δc), height (Δh), weight (Δm_s) and specific gravity (ΔG_s) has been taken to be equal to 0.5 mm, 0.05 mm, 1 g and 0.02, respectively. Using Equation 5, the maximum error in the calculation of the void ratio is in the order of 0.02.

STRESS-STRAIN AND PORE WATER PRESSURE DEVELOPMENT

Stress-strain behavior, pore water pressure development and stress paths for samples with different initial void ratios, consolidated under two effective confining pressures (50 kPa and 300 kPa), are shown in Figures 3 and 4. As can be observed from these figures, even samples with similar void ratios, consolidated at the same confining pressure, show different stress paths, stress-strain behavior and pore water pressure development. For example, test nos. CU5 and CU7 in Figure 3 (void ratios 0.453 and 0.451, respectively) and test nos. CU20 and CU22 in Figure 4 (void ratios 0.479 and 0.471, respectively) show completely different behavior, even though the void ratios are very similar. Some tests show inverse behavior, for example, in Figure 4, test no. CU20 shows strength higher than that of test no. CU22, even though the void ratio of CU22 is lower than that of CU20. Similar trends in soil response could

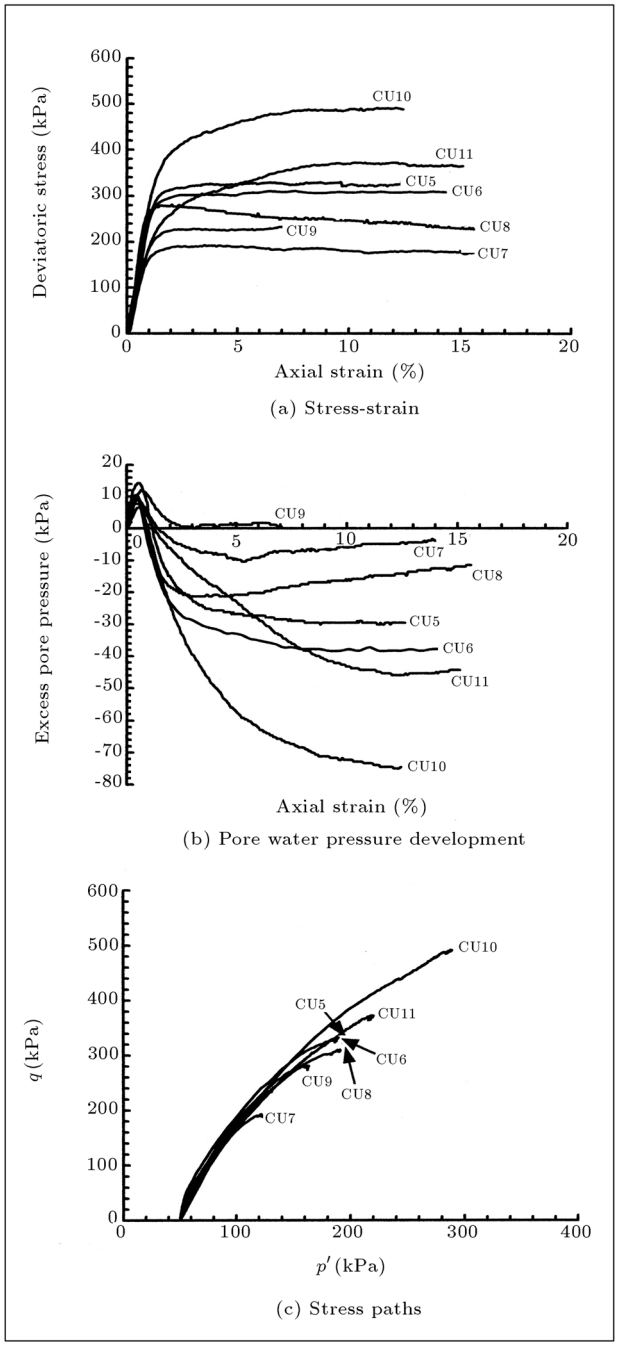

Figure 3. Stress-strain and pore water pressure development for confining pressure 50 kPa.

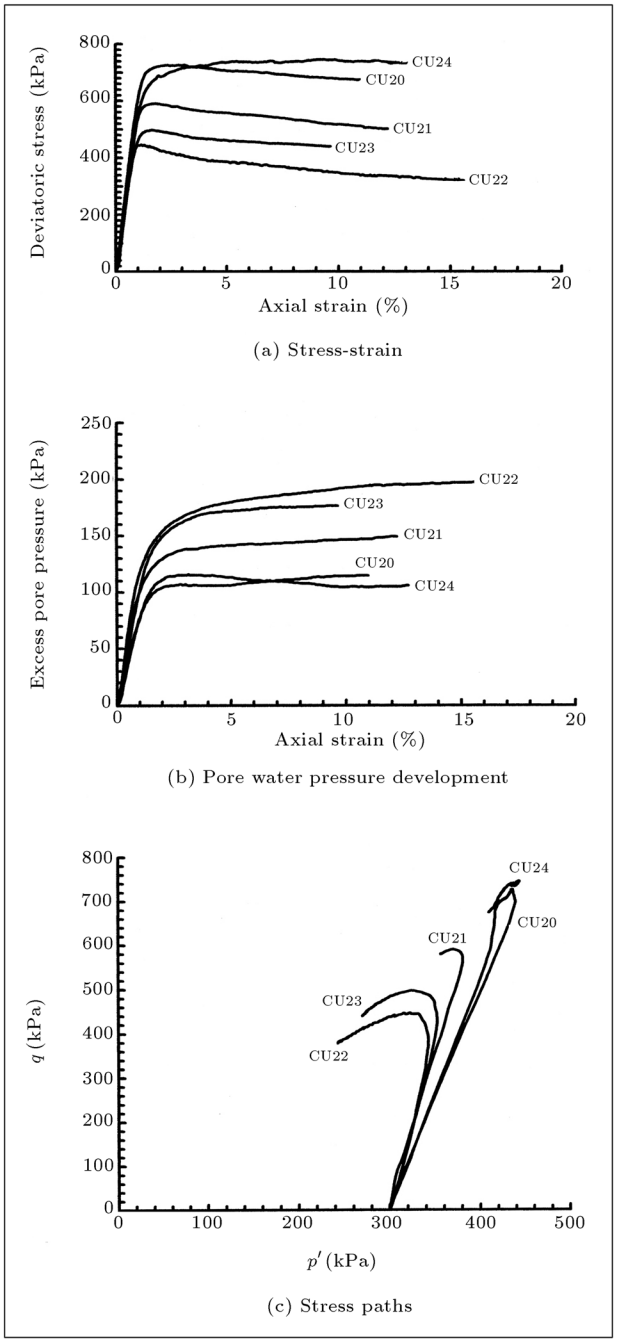

Figure 4. Stress-strain and pore water pressure development for confining pressure 300 kPa.

be observed under other confining pressures. This can be seen more clearly in Figure 5, which shows the stress paths of the tests conducted at all confining pressures on samples prepared at two different relative densities. The stress path of the tests on samples compacted at relative densities of around 50% and 70% are shown in Figures 5a and 5b, respectively. These results show that the behavior of the studied material is dependant on some other parameters, in addition to the void ratio and confining pressure. The test condition and sample preparation techniques were exactly the same for all the tests. However, it is possible for the fabric and structure of the samples, which are unknown, to be different. Although the overall distribution of particle sizes and the overall void ratio were strictly controlled, the arrangement of particles of different size and the distribution of voids within each sample could not be controlled. Chu et al. [20] presents evidence from Verdugo that sample non-uniformity, in terms of grain size distribution, results in completely different behavior. This is also consistent with the fact that small changes of grain size distribution can alter the critical state line of sands significantly. The material studied in this research is not a uniform soil. It includes a wide range of particle sizes, from less than 0.075 mm up to 19 mm. Therefore, the samples may contain different particle arrangements, different void distributions throughout the soil mass, different interparticle forces and different orientations of individual particles. This fabric and structure heterogeneity can affect stress-strain, pore water pressure development and the stress path of the material under triaxial loading.

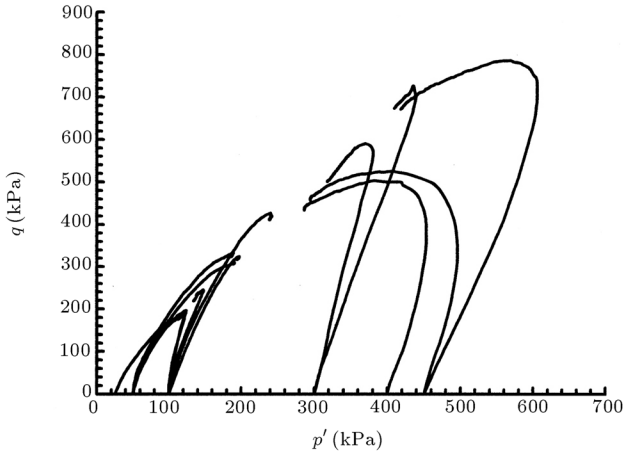

(a) Relative density 50%

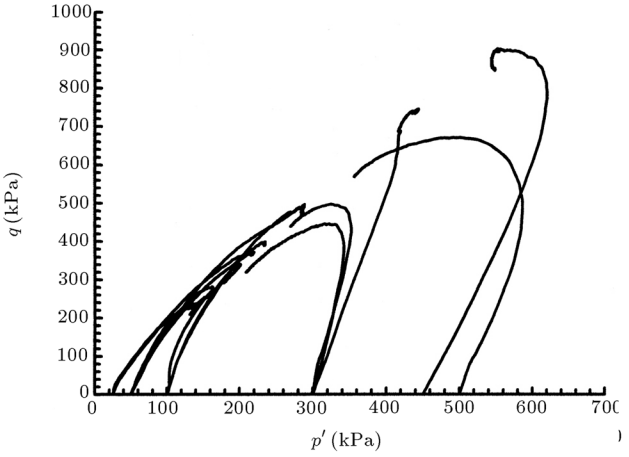

(b) Relative density 70%

Figure 5. Stress paths of all the tests.

Critical State in $q - p'$ Space

Deviatoric stress and pore water pressure at the end of the tests become almost constant, as can be seen from Figures 3 and 4. This suggests that the critical state was reached at the end of each test. The value of q and p' at the end of each test is shown in $q - p'$ space in Figure 6. As can be observed, the state of stresses at the critical state can be represented fairly well by a straight line passing through the origin in $q - p'$ space. The slope of this line, M, equals 1.615. This is equivalent to a critical state angle of friction, (ϕ'_c) of 39.5°.

Critical State in e-ln (p') Space

The paths followed by tests in e-ln (p') space are shown in Figure 7. The changes in p', resulting from pore water pressure changes, can be seen in this figure. It can be seen that the tests starting from low initial confining pressure tend to move to the right (dilative), but, most of the tests at a higher initial confining pressure, after an initial movement to the right, then move to the left (contractive). However, some of the tests at a higher initial confining pressure, still show

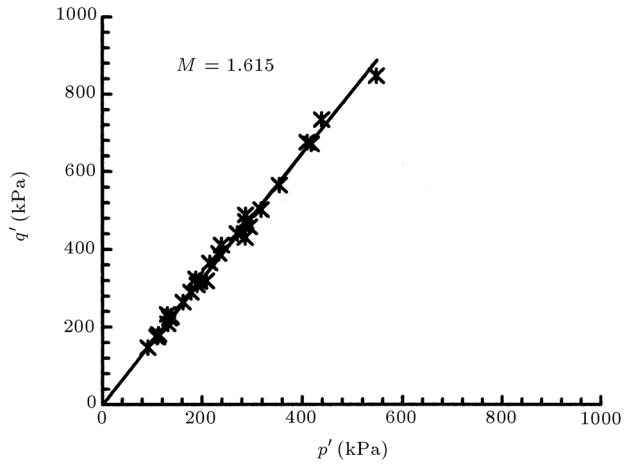

Figure 6. Critical state of tests in $q - p'$ space.

an overall movement to the right, although the trend at the end of the test is to the left.

The critical state line should separate these two types of behavior, the tests to the left of the critical state line showing dilation and those to the right of the critical state line showing contraction. However, as can be observed from Figure 7, the end points of the tests show scatter in e-ln (p') space. This can be seen more clearly from Figure 8, which only shows the void ratio against p' at a critical state. This scatter can be attributed to either error in void ratio calculation and/or variation in soil fabric and structure. As discussed in the previous section, the maximum error in void ratio calculation is $\pm$ 0.02. The difference between the upper and lower limits, in Figure 8, represents a variation of $\pm$ 0.04. Therefore, although errors in void ratio may be one factor in the scatter shown in Figure 8, it is likely that the initial fabric and structure, which form during the remolding of the samples, may also have an effect. Apparently, in a heterogeneous soil mass, initial soil fabric and structure affect the critical state line.

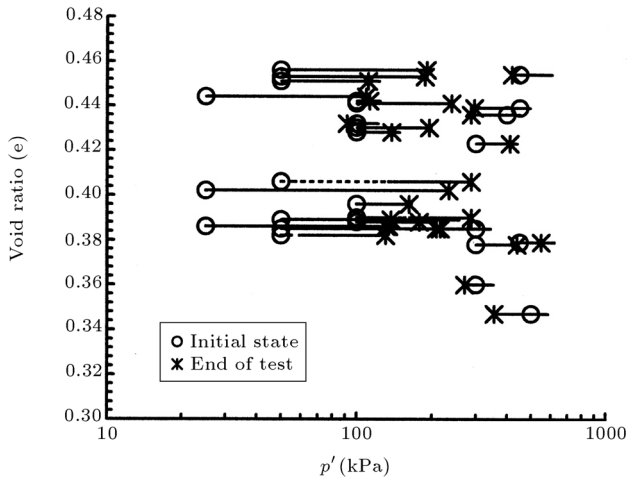

Figure 7. Paths followed by tests in e-ln p' space.

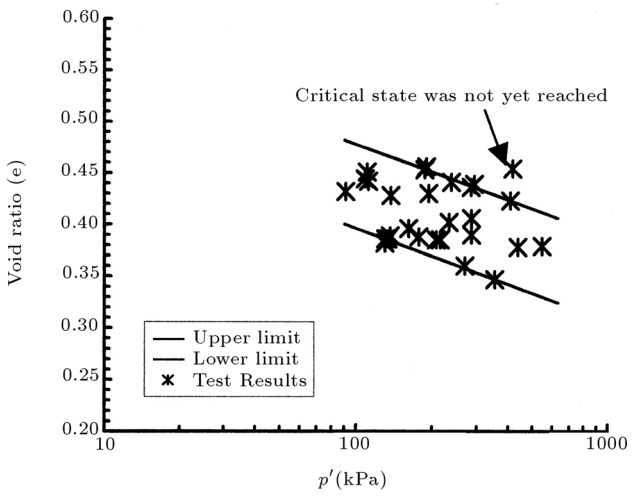

Figure 8. Critical state limits.

This suggests that a unique critical state line can only be defined for a uniform homogeneous soil. This is consistent with the suggestion by Verdugo and Ishihara [9], who have shown that the steady state line is unaffected by the initial fabric, as long as the soil mass is homogeneous. Therefore, for a well graded material, such as gravely sand, where heterogeneity is inevitable, the critical state should be defined as a zone with upper and lower limits, as shown in Figure 8. This fact is consistent with the conclusions presented by other researchers (e.g., [10-14]), who defined the upper and lower limits for the critical state. The critical state limits for gravely sand may be characterized by the following equations as their upper and lower limits in e-ln p':

$$e = 0.657 - 0.039 \ln p' \quad \text{(upper limit)}, \tag{6}$$

$$e = 0.575 - 0.039 \ln p' \quad \text{(lower limit)}. \tag{7}$$

Therefore, for gravely soils, the mean effective stress at critical state, p'_c, can vary between $(p'_c)_{\max}$ and $(p'_c)_{\min}$, corresponding to the upper and lower limits of the critical state zone, depending on the initial fabric and structure.

NORMALIZED STRESS PATHS AND BOUNDARY SURFACES

For comparing data from different tests, it is convenient to normalize the effective stress paths. Three methods have been used for presenting data as the normalized stress path in the literature. Atkinson and Bransby [21,22] describe these three methods. In the first method, p'_e, which is effective mean stress corresponding to the void ratio on the normal consolidation line, is used for normalizing the stress path. This method is not suitable for granular material, because it is difficult to identify the position of the normal consolidation line for granular material. In the second method, p'_c, which is the effective mean stress corresponding to the void ratio on the critical state line, is used for normalization. Since a unique critical state line cannot be defined for this material, it is not possible to simply define a unique p'_c for any void ratio to be used in normalization of the stress paths. For the present paper, a refinement of the second method is used to overcome the difficulty of the critical state being a zone rather than a unique line. Rather than calculating the value of p'_c from an equation for the critical state line, the value of p'_c will be used, and observed for each test, i.e., the mean stress at the end of each test. This means that, by definition, the stress path will reach $p'/p'_c = 1$ at the end of the test.

Figure 9a shows the stress paths in normalized $p'/p'_c - q/p'_c$ space. As can be observed, the stress paths reach different values of q_c/p'_c. Therefore, a normalized deviator stress, defined as $q/(p'_c \times M)$, which was used by Sladen and Oswell [23], can be examined herein as well. Using this method, it follows that all normalized stress paths end at the (1, 1) point, which represents the critical state (Figure 9b). This allows a direct comparison between the behavior of gravely sands having slightly different M values. It can be seen that the normalized stress paths give a clear, consistent picture of the behavior of gravely sand. The critical state is defined by a single point $(p'/p'_c = 1, (q/p'_c)/M = 1)$. Samples with initial p'/p'_c values greater than 0.9, show overall contractive behavior. Although normalized stress paths initially move to the right, they are then bounded by a unique surface (the Roscoe surface) and they follow this surface to reach the critical state. Samples with low p'/p'_c values show dilative behavior and move to the critical state from the left. Samples starting from very low p'/p'_c values (< 0.4) seem to reach a unique boundary surface (the Hvorslev surface), which they then follow to reach the critical state. Samples at intermediate values of p'/p'_c (0.4-0.9) tend to move directly towards the critical state without reaching the boundary surfaces on either side, but the pattern of the stress path direction is still consistent within this region.

The third form of normalization is to use v_λ, as explained by Atkinson and Bransby [21,22]. The data in normalized $q/p' - v_\lambda$ space is shown in Figure 10a. It can be observed that end points of the tests show scatter in this space, because the critical state is a zone rather than a unique line and values of M are slightly different for each test. Therefore, a refinement is introduced in this space to bring all normalized stress paths to the (1, 1) point, to identify the critical state condition. The data is presented in $q/p'/M$ against v_λ/Γ space. Γ is the value of v_λ in the critical state for each test. The data has been plotted in this space and is shown in Figure 10b. Irrespective of different behavior in stress-strain and e-ln p' space, a

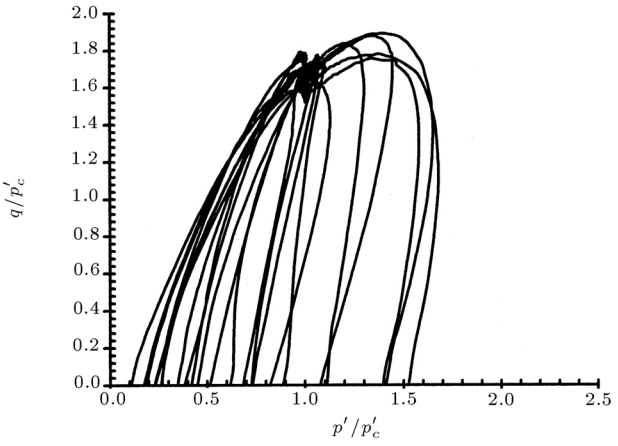

(a) $q/p'_c - p'/p'_c$ space

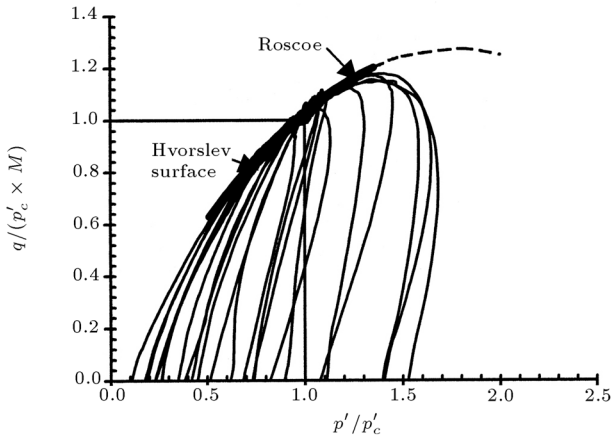

(b) $q/(p'_c \times M) - p'/p'_c$ space

Figure 9. Normalized stress paths.

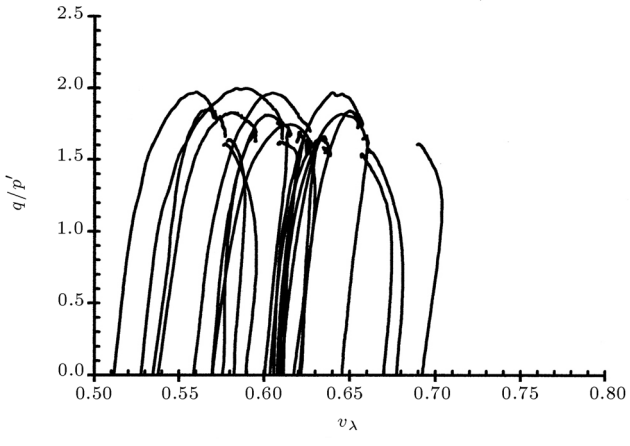

(a) $q/p' - v_\lambda$ space

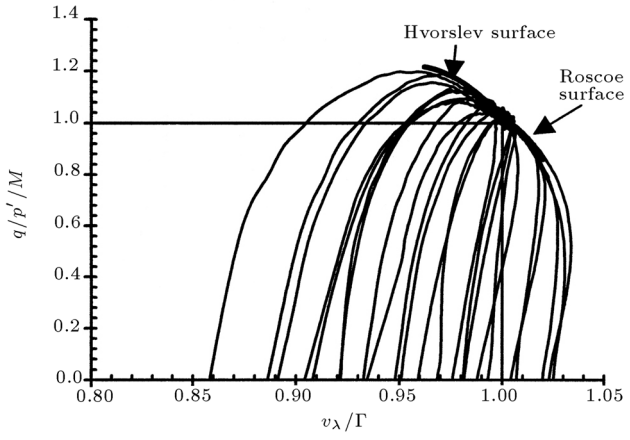

(b) $q/p'/M - v_\lambda/\Gamma$ space

Figure 10. Normalized stress paths.

unique boundary surface can be defined. As with the p'_c normalization, one can see samples on the dense side of the critical state (values of v_λ/Γ less than 0.94) reach a limiting surface (the Hvorslev surface) and see them following that surface down to get to the critical state. Those in a loose state ($v_\lambda/\Gamma >$ 0.99) also reach a limiting surface (the Roscoe surface) and follow that surface up to reach the critical state. Intermediate values of v_λ/Γ (0.94-0.99) tend to move directly towards the critical state without reaching the boundary surfaces on either side, but the pattern of the stress path direction is still consistent everywhere within this region.

CONCLUSION

An extensive series of laboratory tests have been carried out to understand the behavior of gravely sand and to examine critical state concepts for this material. The material studied in this research was a well-graded material and included a wide range of particle size, from less than 0.075 up to 19 mm. For this reason, the samples prepared for triaxial tests are likely to be heterogeneous and can have a different initial soil fabric and structure when prepared at the same void ratio. The results suggest that variations in fabric and structure do affect the behavior of gravely sand. Samples at the same void ratio showed significantly different behavior. The critical state line, defined in $q'-p'$ space, for the gravely sand did not show too large a scatter. However, in e-ln (p') space, the test results did not show a unique critical state line. In this space, a critical state zone with upper and lower limits was defined. Nevertheless, normalizing the behavior, based on the mean stress at the end of each test, allowed the definition of a unique boundary surface. The normalized plot showed a clear, consistent pattern of behavior, with samples on the dense side of the critical state demonstrating dilative behavior (bounded by the Hvorslev surface) and those on the loose state showing contractive behavior (bounded by the Roscoe surface). Plots of $q/(p'_c \times M) - p'/p'_c$ and $q/p'/M - v_\lambda/\Gamma$ have been used to normalize the data to demonstrate this unique behavior. The data showed a unique boundary surface in both normalized spaces.

ACKNOWLEDGMENTS

The triaxial tests were performed in the Soil Mechanics Laboratory of Sharif University of Technology (SUT), with financial support from the Deputy of Research and Technology at SUT, which is acknowledged. The first author gratefully acknowledges the financial support provided by the Ministry of Science, Research and Technology of the Islamic Republic of Iran for his graduate studies, including the visit to Durham University. He also acknowledges the partial funding made available for his visit to Durham University, provided by the British Council.

NOMENCLATURE

e	void ratio
v	specific volume; $v = 1 + e$
q	deviatoric stress; $q = \sigma'_1 - \sigma'_3$
σ'_1	effective major principal stress
σ'_3	effective minor principal stress
p'	mean effective stress; $p' = (\sigma'_1 + 2\sigma'_3)/3$
p'_c	mean effective stress corresponding to critical state line at a defined void ratio (Figure 11)
p'_e	mean effective stress corresponding to normal consolidation line at a define void ratio (see Figure 11)
λ	slope of critical state line in v-lnp' space (see Figure 11)
v_λ	specific volume on the reference section at $p' = 1$ KN/m^2 (see Figure 11): $v_\lambda = v + \lambda \ln p'$
Γ	v_λ corresponding to p'_c (see Figure 11); $\Gamma = v + \lambda \ln p'_c$
V_0	initial volume of the sample
V_m	volume change due to membrane penetration
V_c	volume of the sample after consolidation
M	slope of critical state line in stress space

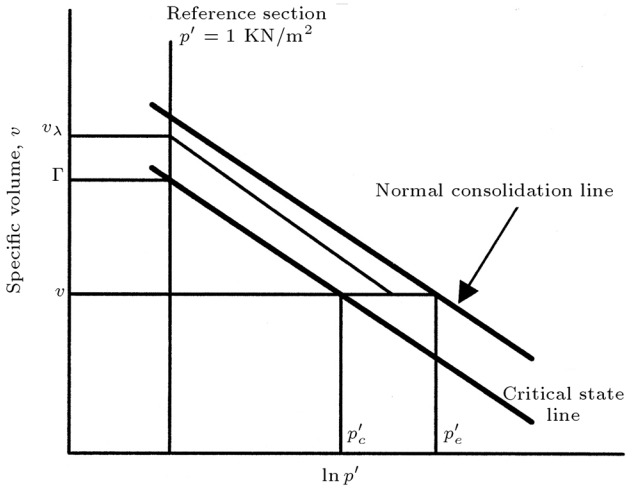

Figure 11. Schematic diagram showing definition of symbol and notation.

REFERENCES

1. Casagrande, A. "Characteristics of cohesionless soils affecting the stability of earth fills", *J. Boston Soc. Civ. Engrs.*, Reprinted in contribution to soil mechanics 1925-1940, Boston Society of Civil Engineers, USA (1936).
2. Taylor, D.W., *Fundamentals of Soil Mechanics*, John Wiley & Sons, New York, USA (1948).
3. Roscoe, K.H., Schofield, A.N. and Wroth, C.P. "On the yielding of soils", *Geotechnique*, **8**(1), pp 22-53 (1958).
4. Schofield, A.N. and Wroth, C.P., *Critical State Soil Mechanics*, McGraw-Hill, London, UK (1968).
5. Poulos, S.J. "The steady state of deformation", *J. Geotech. Engrg. ASCE*, **107**, GT5, pp 553-562 (1981).
6. Been, K., Jefferies, M.G. and Hachey, J. "The critical state of sands", *Geotechnique*, **41**(3), pp 365-381 (1991).
7. Chu, J. "An experimental examination of the critical state and other similar concepts for granular soils", *Can. Geotech. J.*, **32**(6), pp 1065-1075 (1995).
8. Riemer, M.F. and Seed, R.B. "Factors affecting apparent position of steady-state line", *J. Geotech. Engrg. ASCE*, **123**(3), pp 281-288 (1997).
9. Verdugo, R. and Ishihsra, K. "The steady state of sandy soils", *Soils & Foundations*, **36**(2), pp 81-91 (1996).
10. Fourie, A.B. and Papageorgiou, G. "Defining an appropriate steady state line for Merriespruit gold tailings", *Can. Geotech. J.*, **38**(4), pp 695-706 (2001).
11. Yamamuro, J.A. and Lade, P.V. "Steady-state concepts and static liquefaction of silty sands", *J. Geotech. Engrg. ASCE*, **124**(9), pp 868-877 (1998).
12. Mooney, M.A., Finno, R.J. and Viggiani, M.G. "A unique critical state for sands?", *J. Geotech. Engrg. ASCE*, **124**(11), pp 1100-1108 (1998).
13. Konrad, J.M. "Minimum undrained strength of two sands", *J. Geotech. Engrg. ASCE*, **116**(6), pp 932-947 (1990).
14. Konrad, J.M. "Minimum undrained strength versus steady-state strength of sands", *J. Geotech. Engrg. ASCE*, **116**(6), pp 948-963 (1990).
15. Konrad, J.M. "Undrained response of loosely compacted sands during monotonic and cyclic compression tests", *Geotechnique*, **43**(1), pp 69-89 (1993).
16. Baldi, G. and Nova, R. "Membrane penetration effects in triaxial testing", *J. Geotech. Engrg. ASCE*, **110**(3), pp 403-420 (1984).
17. Ansal, A.M. and Erken, A. "Posttesting correction procedure for membrane compliance effects on pore pressure", *J. Geotech. Engrg. ASCE*, **122**(1), pp 27-38 (1996).
18. Nicholson, P.G., Seed, R.B. and Anwar, H.A. "Elimination of membrane compliance in undrained triaxial testing", *I. Measurement and Evaluation, Can. Geotech. J.*, **30**, pp 727-738 (1993).
19. Vaid, Y.P. and Sivathayalan, S. "Errors in estimates of void ratio of laboratory sand specimens", *Can. Geotech. J.*, **33**(6), pp 1017-1020 (1996).
20. Chu, J., Lo, S.C.R., Been, K., Jefferies, M.G., Hachey, J., Verdugo, R., Vaid, Y.P. and Pillai, V.S. "The critical state of sands-discussion", *Geotechnique*, **42**(4), pp 655-663 (1992).
21. Atkinson, J.H. and Bransby, P.L., *The Mechanics of Soils*, McGraw-Hill, London, UK (1978).
22. Atkinson, J.H., *An Introduction to the Mechanics of Soils and Foundations*, McGraw-Hill, London, UK (1993).
23. Sladen, J.A. and Oswell, J.M. "The behavior of very loose sand in the triaxial compression test", *Can. Geotech. J.*, **26**(1), pp 103-113 (1989).